Advanced Mo-based Rare process Experiment

Status and perspectives of the AMoRE experiment

Vladimir Kazalov

on behalf of the AMoRE Collaboration

Baksan Neutrino Observatory

INR RAS

The 22nd Lomonosov Conference
Moscow, 2025

vvk1982@mail.ru

AMoRE collaboration

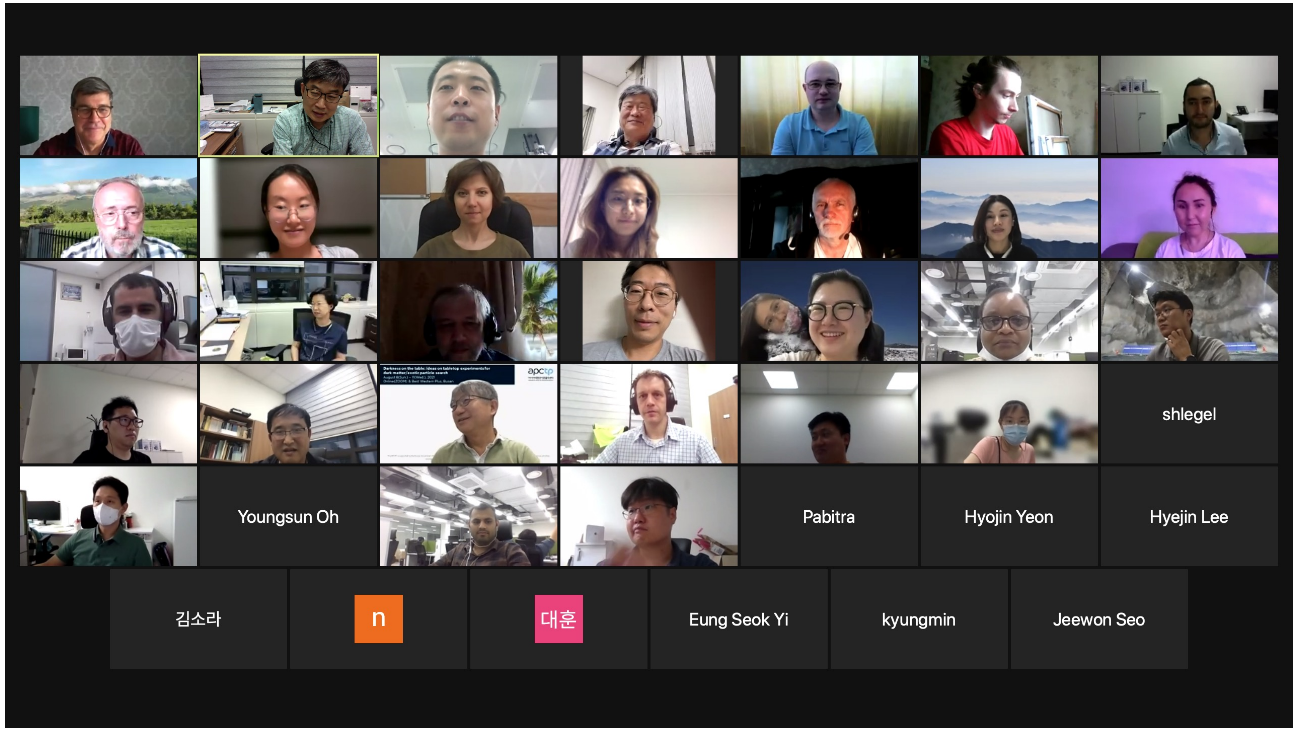

10 Countries, 26 Institutions - Korea, Germany, Ukraine, USA, Russia, China, Thailand, Indonesia, India, Pakistan

The AMORE-experiment's challenge

The goal of the **AMoRE** (**A**dvanced **Mo**-base **R**are process **E**xperiment) is to search for neutrinoless double beta decay (0υββ) of ^{100}Mo using Mo-based scintillating crystals and low-temperature sensors.

Experimental signature of 2vββ and 0vββ:

$$^{100}Mo \xrightarrow{2\nu\beta\beta} {}^{100}Ru + 2\beta^- + \bar{\nu}_e$$

$$^{100}Mo \xrightarrow{0\nu\beta\beta} {}^{100}Ru + 2\beta^-$$

$2\nu\beta\beta$ decay
- 2^{nd} order beta decay
- Rare nuclear decay
- ($>10^{18}$ years of half life)

$0\nu\beta\beta$ decay
- Massive neutrino
- Majorana particle
- Beyond the SM model
- $>10^{25}$ years of half-life

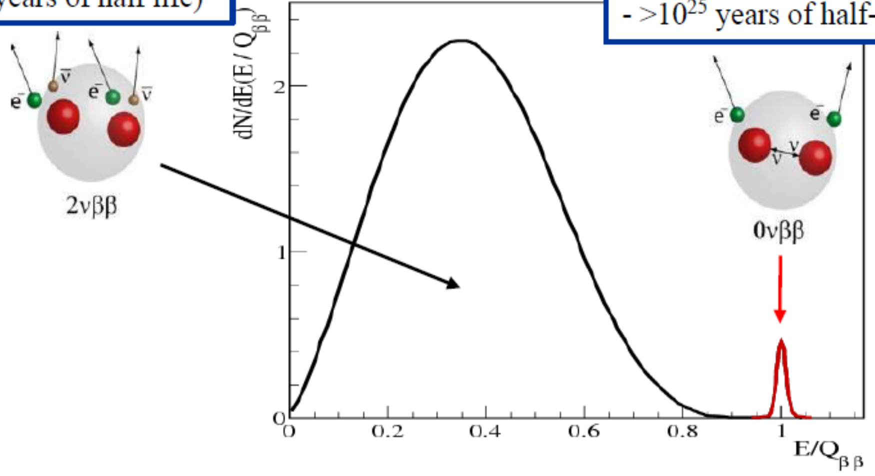

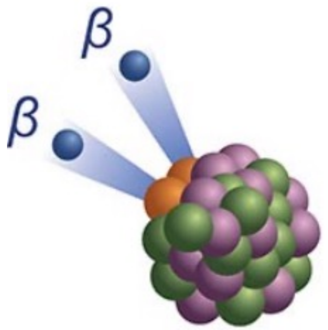

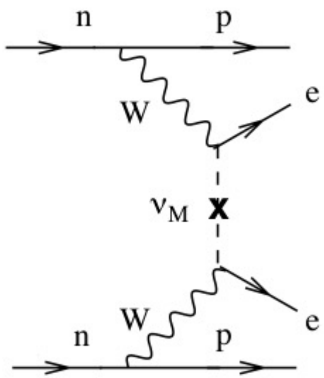

To observe 2vββdecay, the single β-decay must be energetically forbidden due to energy conservation constraint.

In total 35 isotopes available and > 9 of them can be used for 0vββ search.

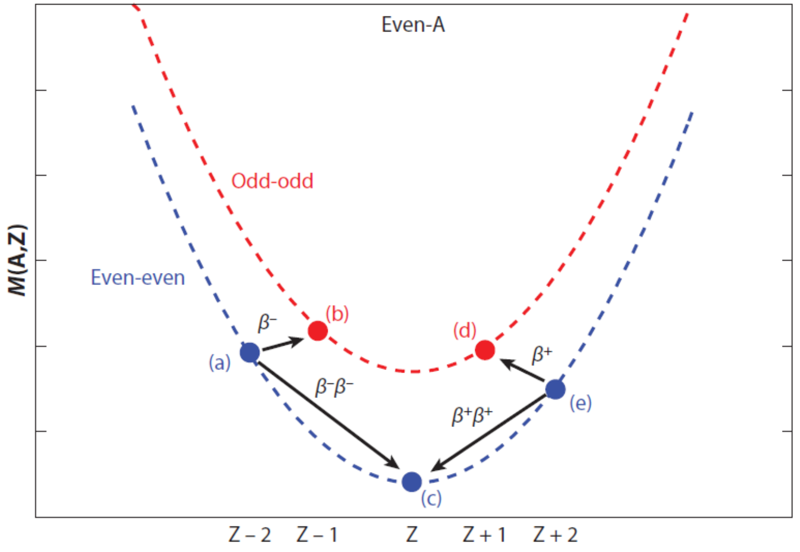

- Lepton-number violation (**ΔL=2**)
- The nature of neutrino mass (**Dirac or Majorana?**)
- Type of neutrino mass hierarchy (normal, inverted)
- CP-violation in the lepton sector

Why ^{100}Mo is chosen for 0υββ experiment

- ✓ **High Q-value of 3034,34 keV**
- ✓ **High natural abundance of 9.7%**
- ✓ **Relatively short half-life (0υββ) expected from theoretical calculation**

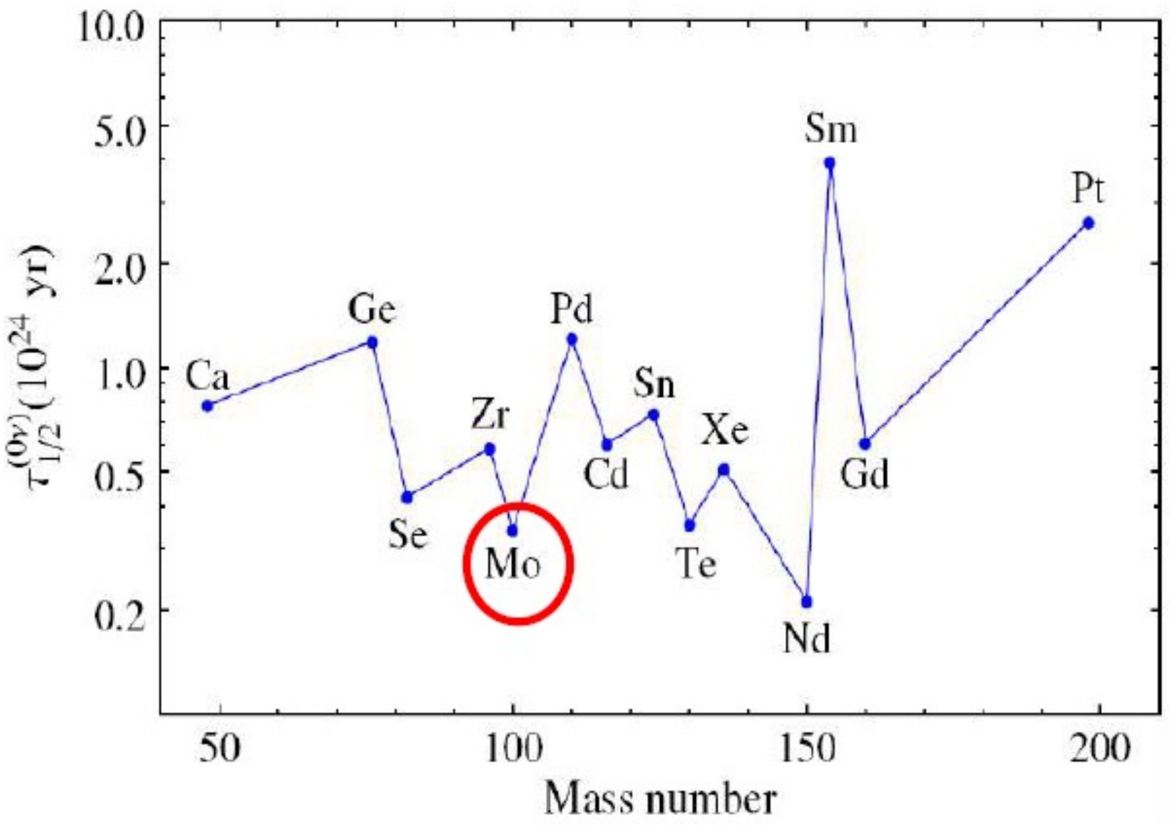

Barea et al., Phy. Rev. Lett. 109, 042501 (2012)

Isotope	Q (MeV)	Abund. %
^{48}Ca	4,271	0,19
^{76}Ge	2,040	7,8
^{82}Se	2,995	8,7
^{96}Zr	3,35	2,8
^{100}Mo	3,034	9,7
^{116}Cd	2,802	7,5
^{124}Sn	2,228	5,8
^{130}Te	2,533	34,1
^{136}Xe	2,479	8,9
^{150}Nd	3,367	5,6

AMoRE experimental campaigns

AMoRE-pilot

2015-2018

6 $^{48dep}CaMoO_4$ crystals:
1.9 (0.88) kg of CMO (^{100}Mo)
Yangyang Underground Lab
(Y2L, 700 m depth)

ν-2022

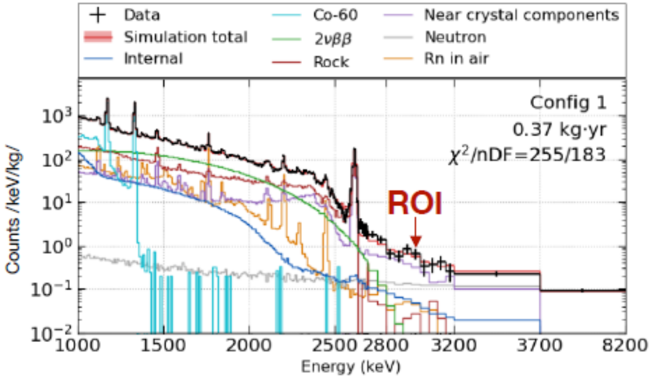

- Live exposure ~ 0.32 $kg_{Mo\text{-}100}$·yr.
- Background at ROI
  ~0.5 cnts/keV/kg/year.
- $T^{0\nu}_{1/2} > 3.2 \times 10^{23}$ yrs (90% CL)

Astropart. Phys. 162 102991 (2024)
EPJC 79:791 (2019)

AMoRE-I

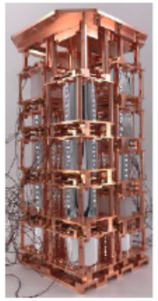

2020-2023

13 CMOs
+ 5 Li_2MoO_4 crystals :
6.2 (3.0) kg of XMO (^{100}Mo)
Y2L

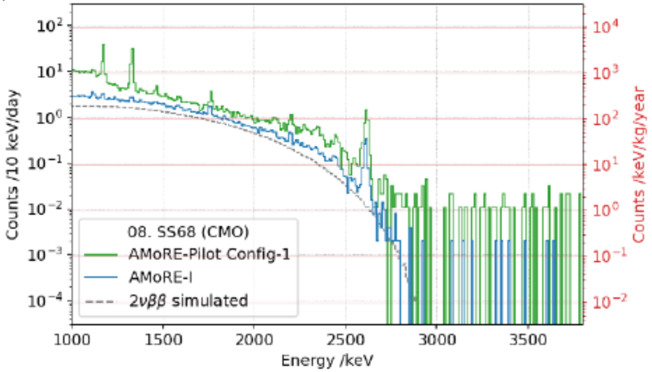

- Live exposure ~ 4 $kg_{Mo\text{-}100}$·yr.
- Background at ROI~0.025 ckky.
- $T^{0\nu}_{1/2} > 2.9 \times 10^{24}$ yrs (90% CL)
- World best limit for $0\nu\beta\beta$ of ^{100}Mo.

PRL 134 082501 (2025)

AMoRE-II

2025-

Stage 1:
90 LMOs
(27 kg)

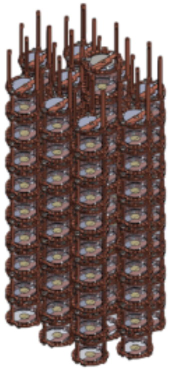

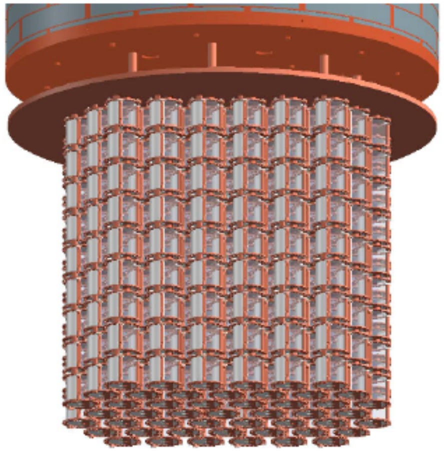

Stage 2:
360 crystals (157 kg)

- ~ 90 kg of ^{100}Mo
- In Yemilab, 1000 m depth.
- Exposure > 500 $kg_{Mo\text{-}100}$·yr.
- Background at ROI~10^{-4} ckky.
- Aiming at $T^{0\nu}_{1/2} \sim 4.5 \times 10^{26}$ yrs

Production of ^{100}Mo and ^{48depl}Ca

- **Production of the ^{100}Mo isotope:**
  - JSC "PO Electrochemical Plant" (ECP), Krasnoyarsk, Russia
  - $^{100}MoO_3$ powder:
    - → ^{100}Mo enrichment: ~ 95%
    - → Radioactive purity:

ICP-MS at CUP	U: ~ 0.2 ppb	Th: ~ 0,05ppb
HPGe at BNO INR RAS	^{226}Ra: ≤ 8 mBq/kg	^{228}Ac: ≤ 3.5 mBq/kg

- **Calcium carbonate (calcium formate) enriched by ^{40}Ca and depleted by ^{48}Ca:**
  - Elektrokhimpribor (EKP), Lesnoy, Russia
  - $^{40}CaCO_3$ powder:
    - ^{48}Ca < 0,001%
    - Radioactive purity: U ≤ 0.1 ppb, Th ≤ 0,1 ppb, Sr= 1 ppm, Ba = 1 ppm, ^{226}Ra = 5 mBq/kg (late samples from NEOHIM 1.4 mBq/kg), ^{228}Ac (228Th) = 1 mBq/kg

- **Lithium carbonate (old USSR)**

$^{48depl}Ca^{100}MoO_4$ and $Li_2{}^{100}MoO_4$ crystals

- $^{48depl}Ca^{100}MoO_4$ – production of JSC "FOMOS-Materials“
  13 crystals, AMoRE-pilot, AMoRE-I

- $Li_2{}^{100}MoO_4$ – grow by Institute of Inorganic Chemistry SB RAS NIIC, (Low temp. gradient), AMoRE-I, AMoRE-II

- $Li_2{}^{100}MoO_4$ – grow by Center for Underground Physics (CUP) (Czochralski method)

Absolute light yield of CMO crystals:

~ 4,900 ph/MeV, at room temperature, (H.J. Kim et al., IEEE TNS 57 (2010) 1475)
~ 30000 ph/MeV at a temperature of 10 mK

CMO crystals have the highest light yield among Mo-containing crystals.

6 Pilot CMOs

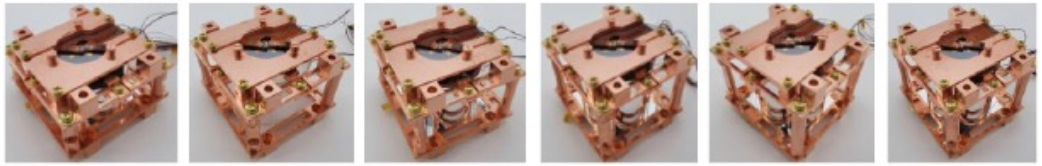

7 New CMOs

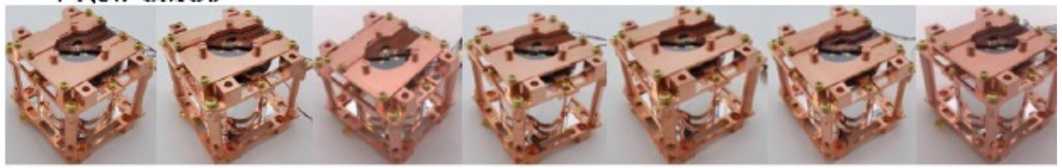

5 New LMOs

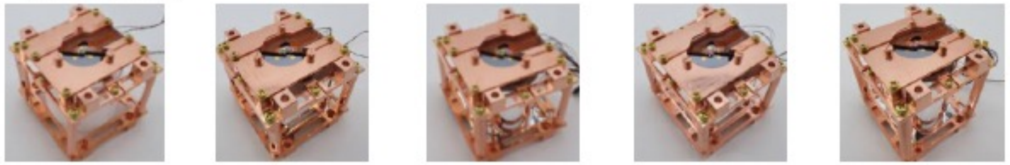

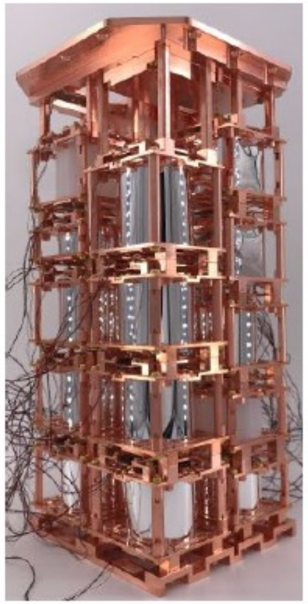

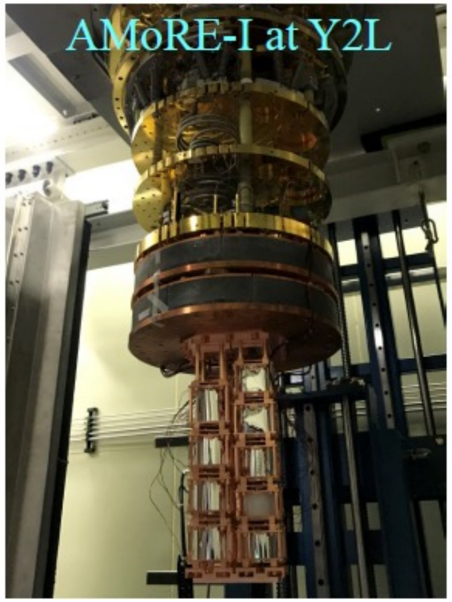

Principle of AMoRE detector

Scintillating crystal
- $^{48depl}Ca^{100}MoO_4$
- ^{100}Mo enriched: > 95 %
- ^{48}Ca depleted: < 0.001 %

MMC & SQUID
- MMC: Metallic Magnetic Calorimeter
- Magnetization changes with temperature.
- Magnetization change (flux) can be measured as a voltage by SQUID

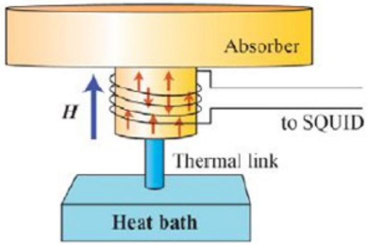

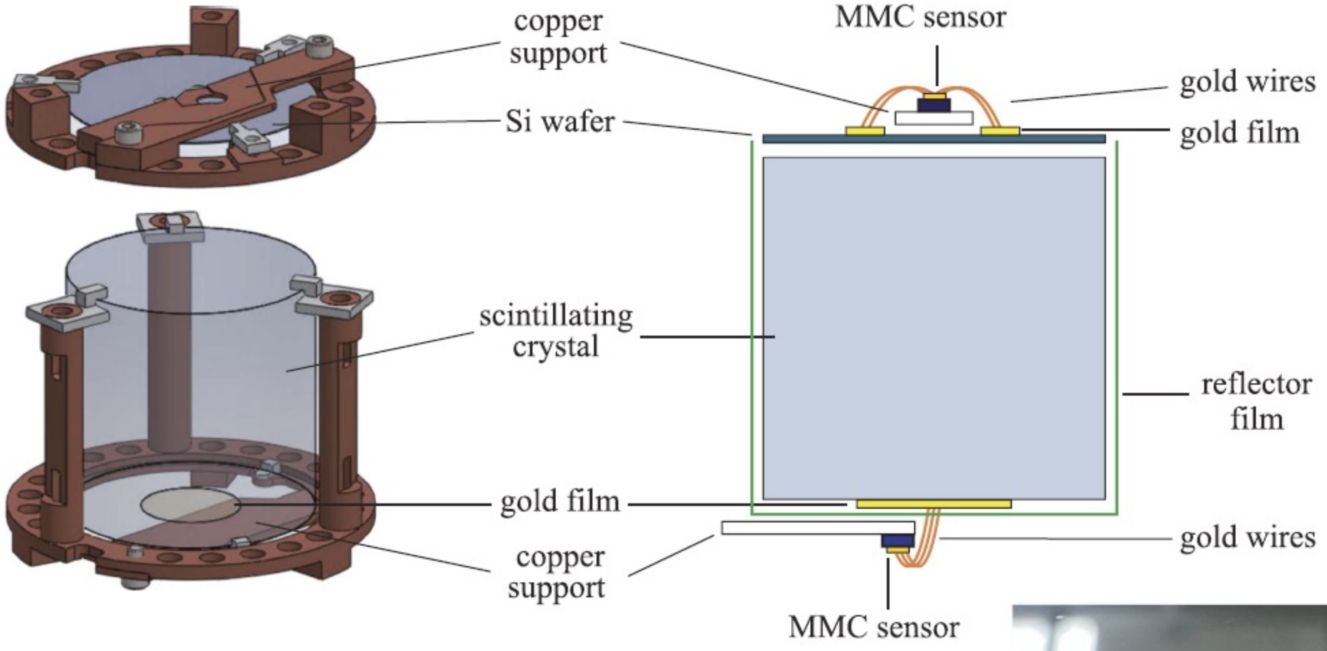

Detection process:
Energy → Temperature → Magnetization → Magnetic flux → **Voltage**

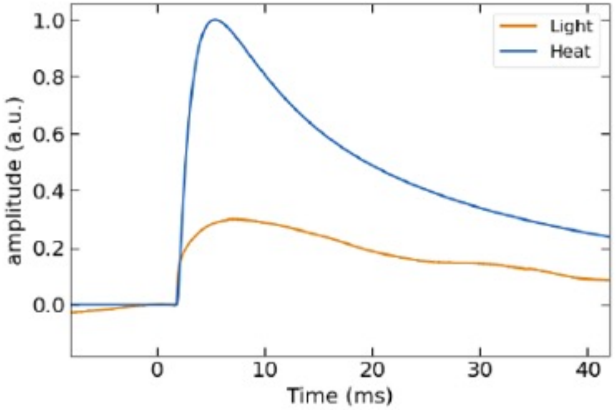

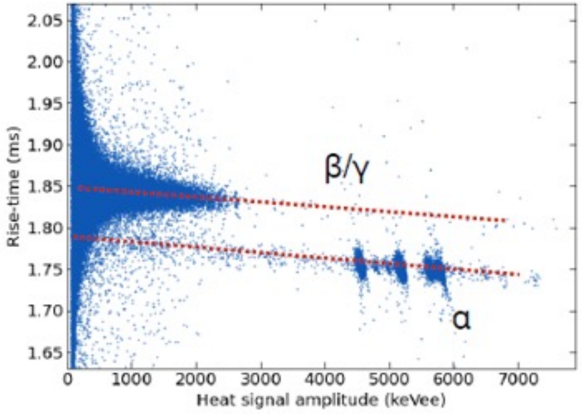

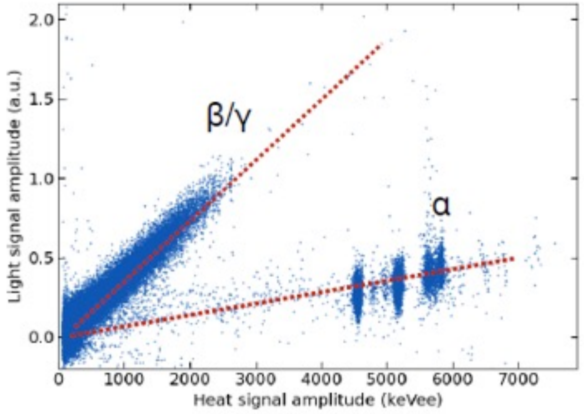

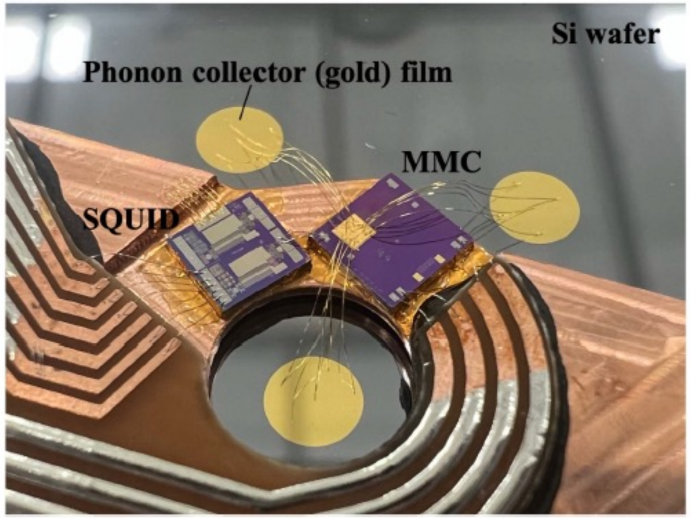

Signal processing and analysis

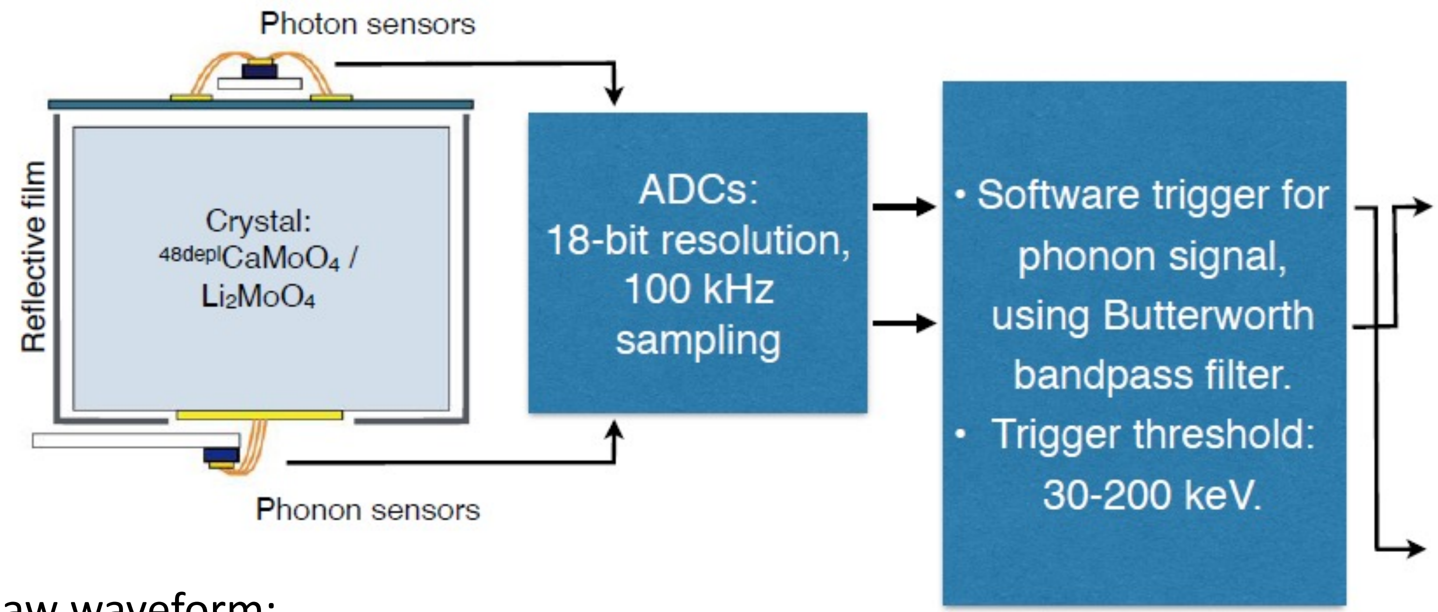

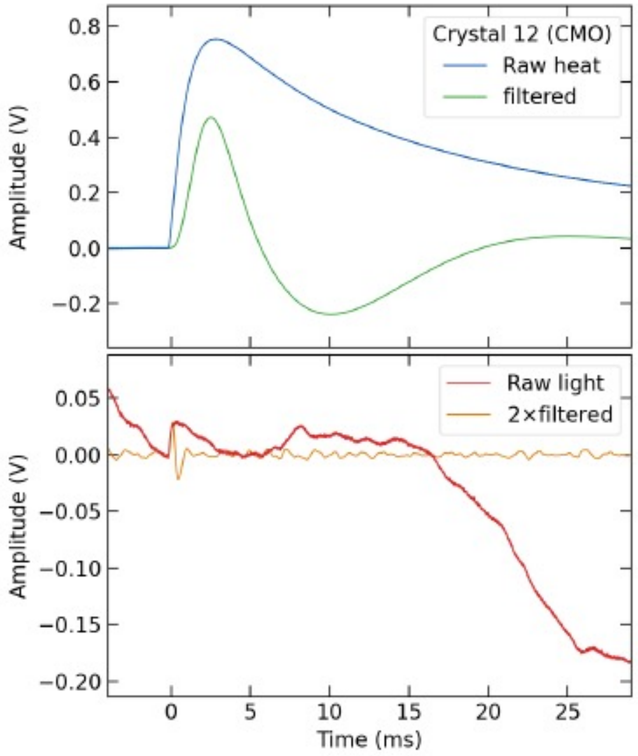

- Raw waveform:

- baseline/noise information
- timings (rise/fall): pulse shape discrimination (PSD)

Reconstruction for improving energy resolution and β/α discrimination power (DP):

-Butterworth bandpass filter— mainly for noise suppression:

- pulse amplitude: pulse height or a least square fit to the template signal.

- Stabilization heater signal for gain drift corrections.

Particle Identifications, CMO and LMO

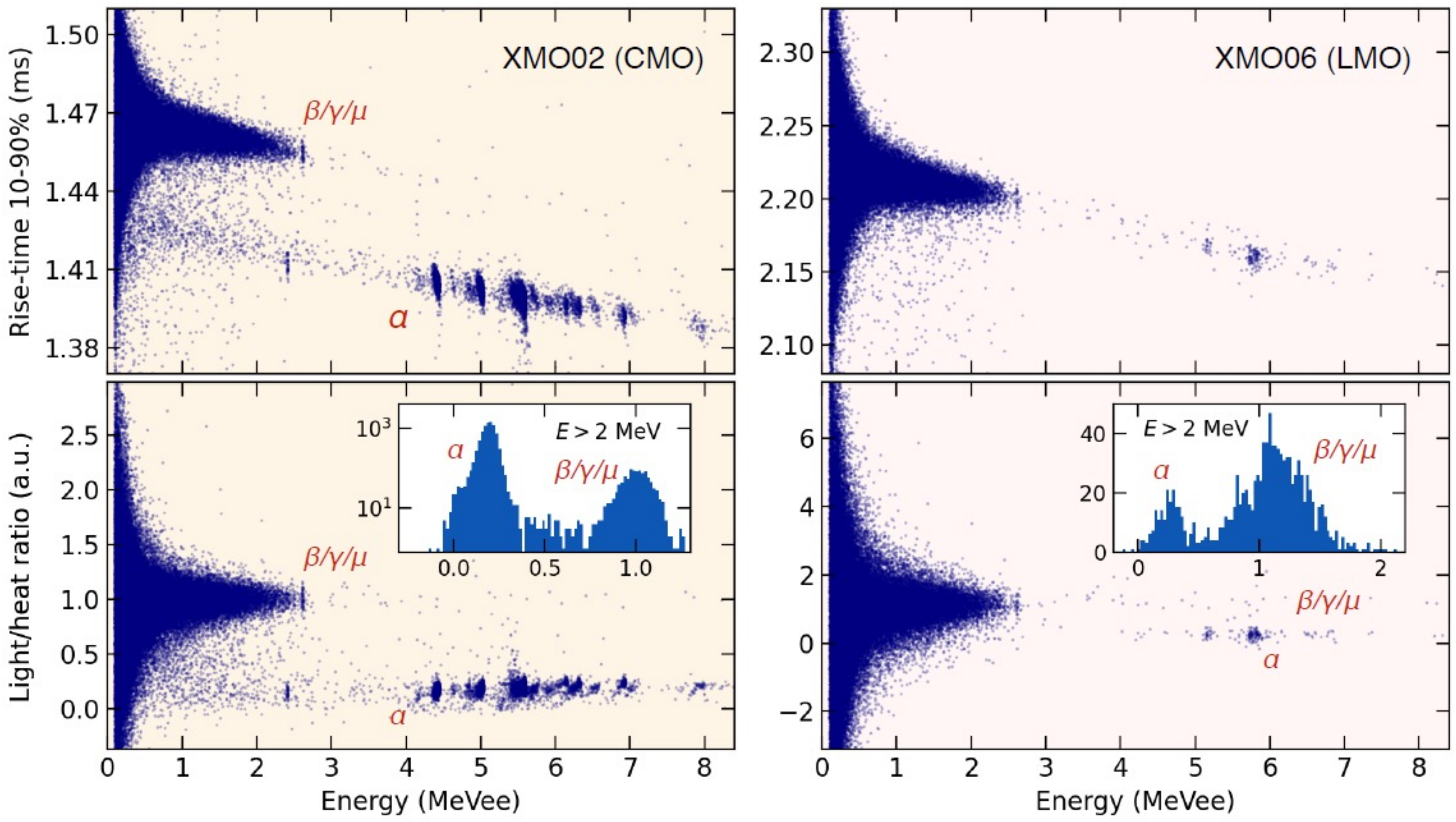

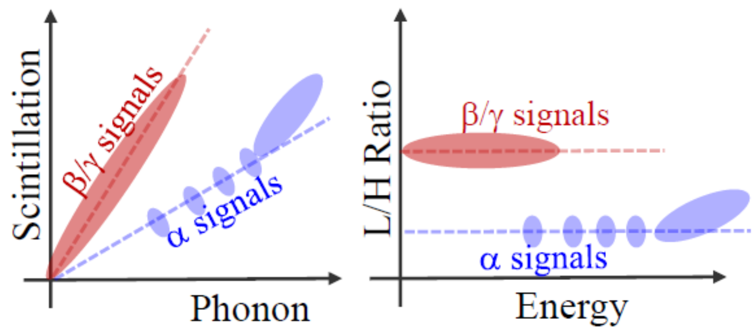

Simultaneous heat & light measurements

- Particle discrimination for rejection of α-induced background

Discrimination Power (DP):

$$DP \equiv \frac{|\mu_{\beta/\gamma} - \mu_\alpha|}{\sqrt{\sigma_{\beta/\gamma}^2 + \sigma_\alpha^2}}$$

μ - the mean value of the distribution

σ - standard deviation of this distribution

- CMO shows better discrimination power — light yield: CMO > LMO.
- LMO has much less α contamination.

Particle Identifications, CMO and LMO

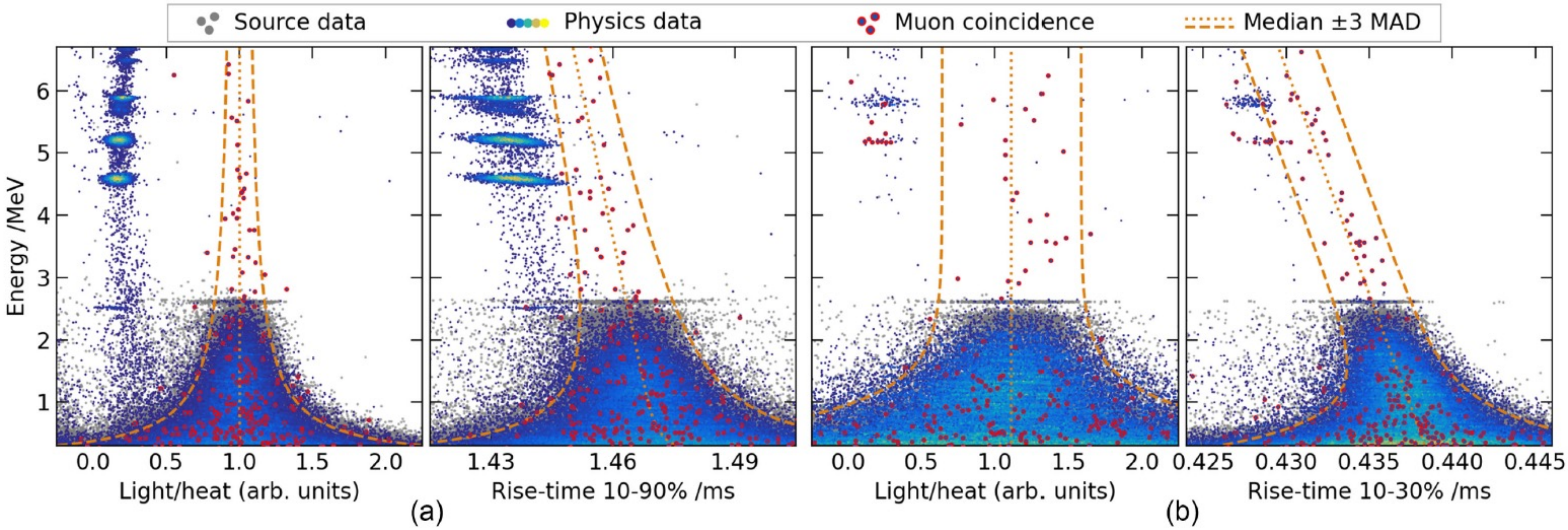

Particle discrimination parameters: light-to-heat ratios (L/H) and the raw heat signals' RTs of (a) a CMO and (b) an LMO detector. Dots with blue-yellow color gradients denote physics data, overlaid on the source data denoted as gray dots. Events in both 3-MAD bands for L/H and RT denoted as dashed-orange curves were selected as β/γ events. Events in the muon veto window are indicated by red circles. Some α-like events with muon coincidence at the electron equivalent energy slightly above 5 MeV in the LMO data are caused by the capture of muon-induced neutrons on the lithium-6 nuclei: $^{6}Li(n,\alpha)t$.

Phys.Rev.Lett. 134 (2025) 8, 082501

Energy calibration

Calibration source: ^{232}Th-rich welding rods just outside of OVC.

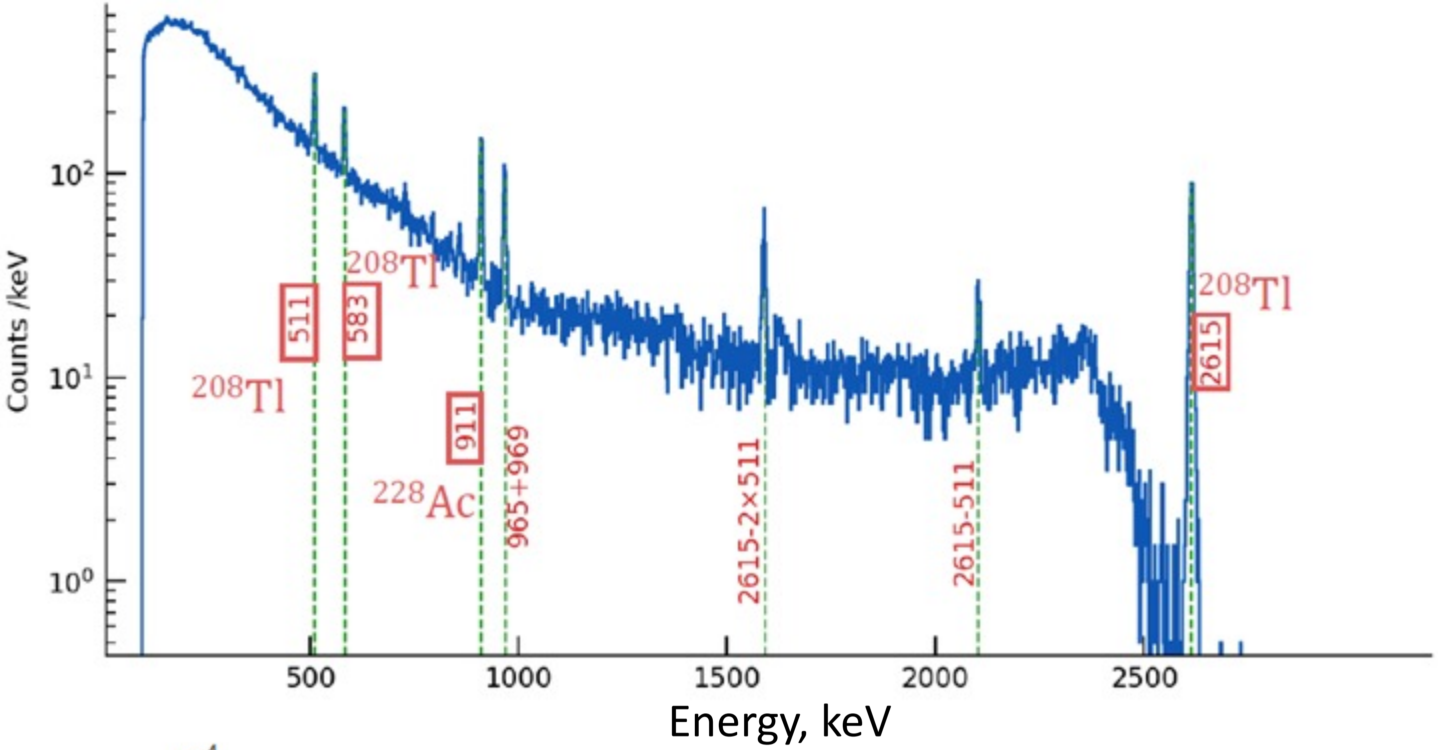

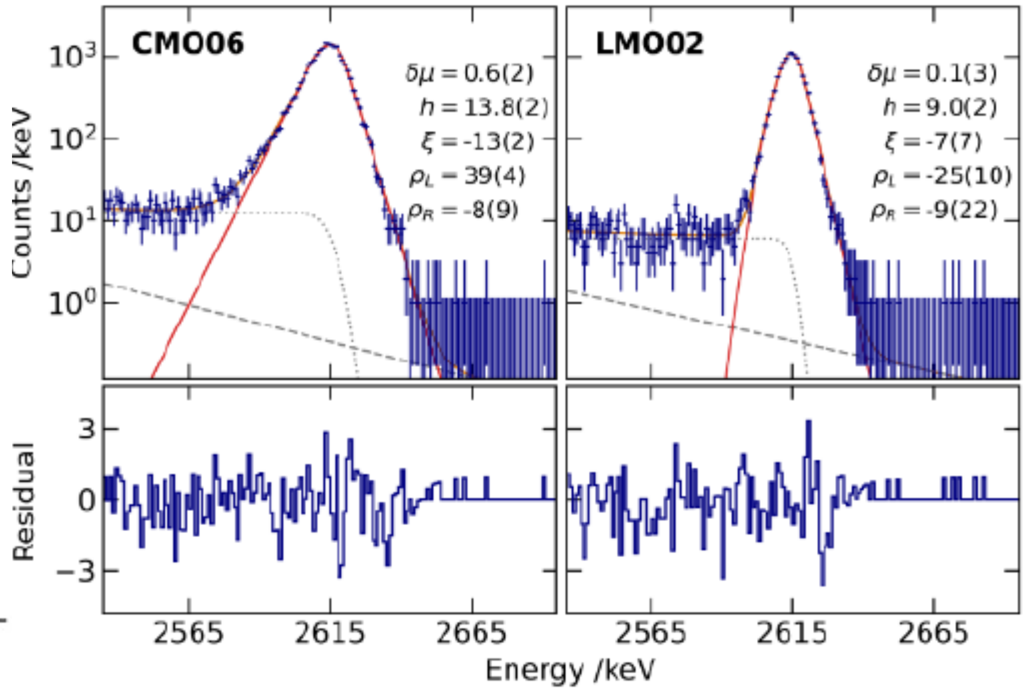

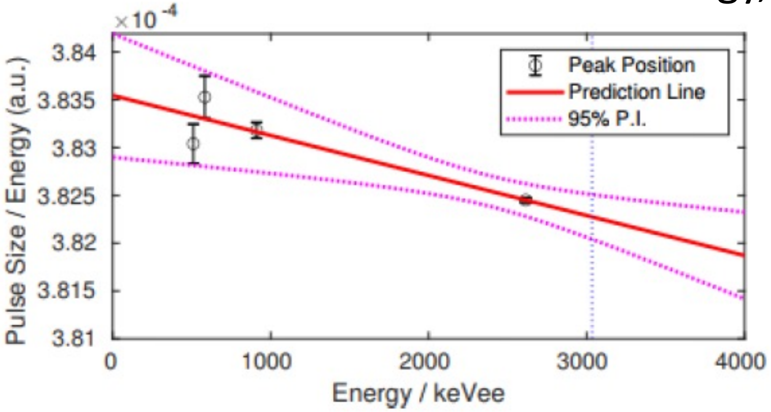

- Asymmetric gaussian (Bukin) function to describe γ-peaks
- Quadratic polynomial calibration
- Slight non-linearity

AMoRE-I experimental setup

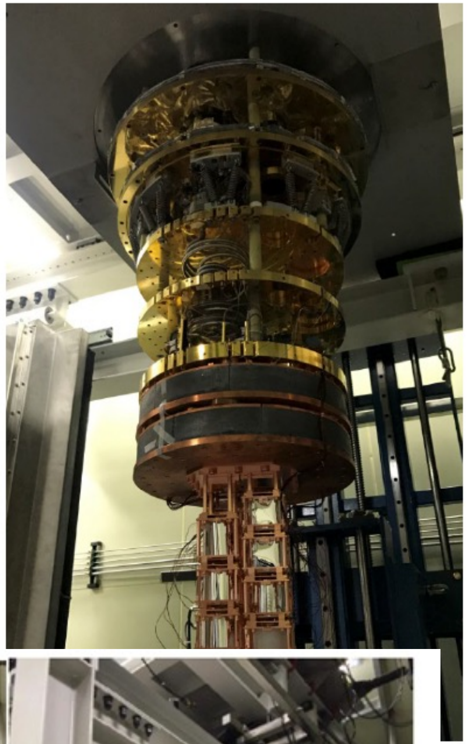

with superconducting shield

- 18 crystals: 13 $^{48depl}Ca^{100}MoO_4$ (4.58 kg) + 5 $Li_2{}^{100}MoO_4$ (1.61 kg)
- Total crystal mass 6.19 kg (3.0 kg ^{100}Mo)
- MMC sensor: Au:Er ➔ Ag:Er
- Using same cryostat + two-stage temperature control: $\langle \Delta T \rangle < 1\ \mu K$
- Shielding enhancements:
  - Outer Pb: 15 ➔ 20 cm; neutron shields
  - boric acid silicon + more PE / B-PE
  - More muon counter coverage
  - More supply of Rn-free air.

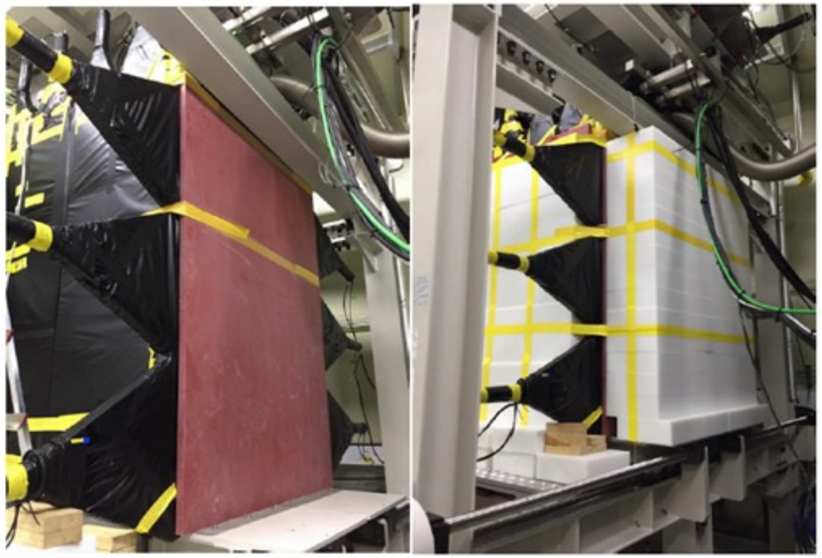

Outside of detector
(Borated PE & PE)

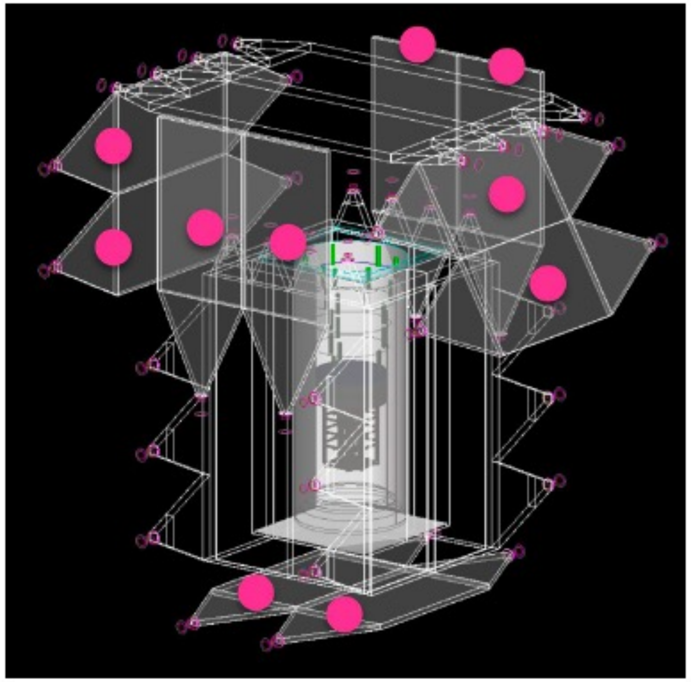

YangYang Underground Laboratory (Y2L)

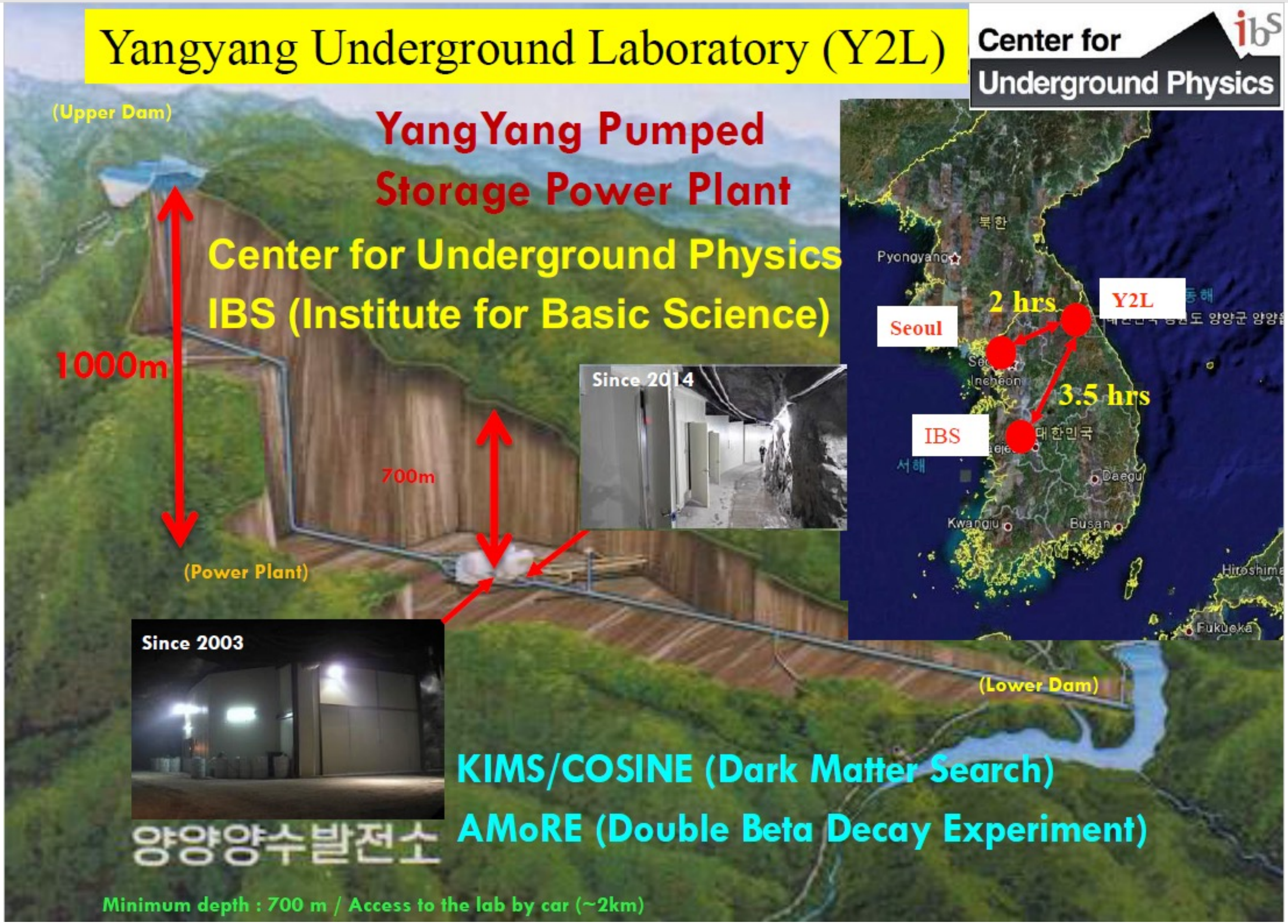

Background spectra AMoRE-I after alpha background rejection

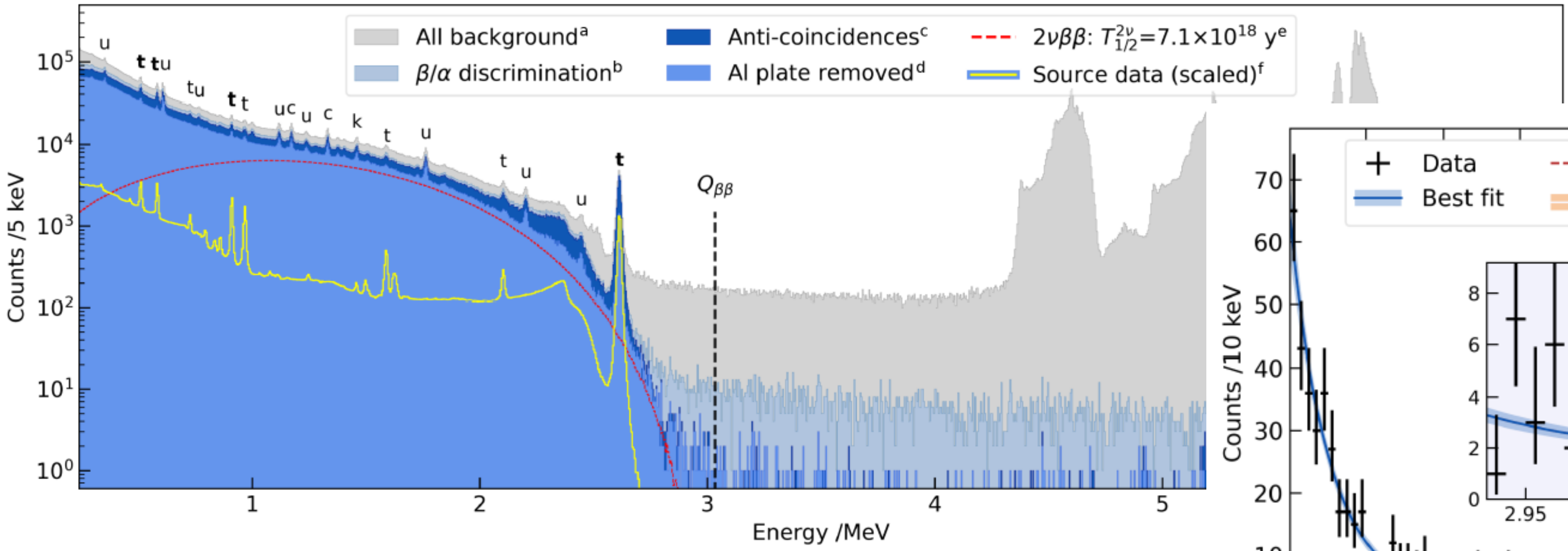

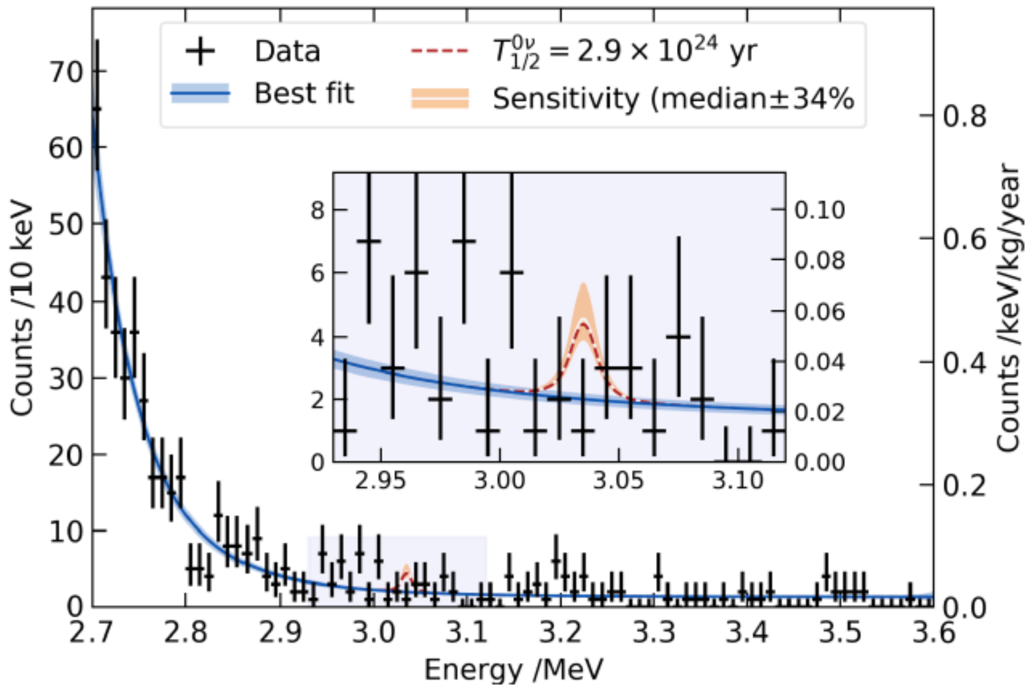

- 17 crystals excluding one LMO (for very poor β/α discrimination power)
  Exposure = 8.02 kgXMoO4 · yr = 3.88 kg^{100}Mo · yr.

CMO has higher alpha backgrounds and rejection power is high

LMO has lower alpha backgrounds and rejection power is low

^{100}Mo 0νββ limit from AMoRE-I: $T^{0\nu\beta\beta}_{1/2} > 2{,}9\times10^{24}$ *years* (90% *C.L.*)(**$m_{\beta\beta}$<210−610 meV**)

Improved Limit on Neutrinoless Double Beta Decay of ^{100}Mo from AMoRE-I
Phys.Rev.Lett. 134 (2025) 8, 082501

The best limit for 0νββ of ^{100}Mo before AMoRE-I was obtained by CUPID-Mo - 1.8×10^{24} years (90% C.L.)

AMoRE-II @Yemilab

- Yemilab is constructed in 2022. (1000m deep)
- Lab space > 3000 m^2 , 2.5 MW electricity.
- Two access ways: ramp-way, men-riding cage
- Open to other researchers IBS.

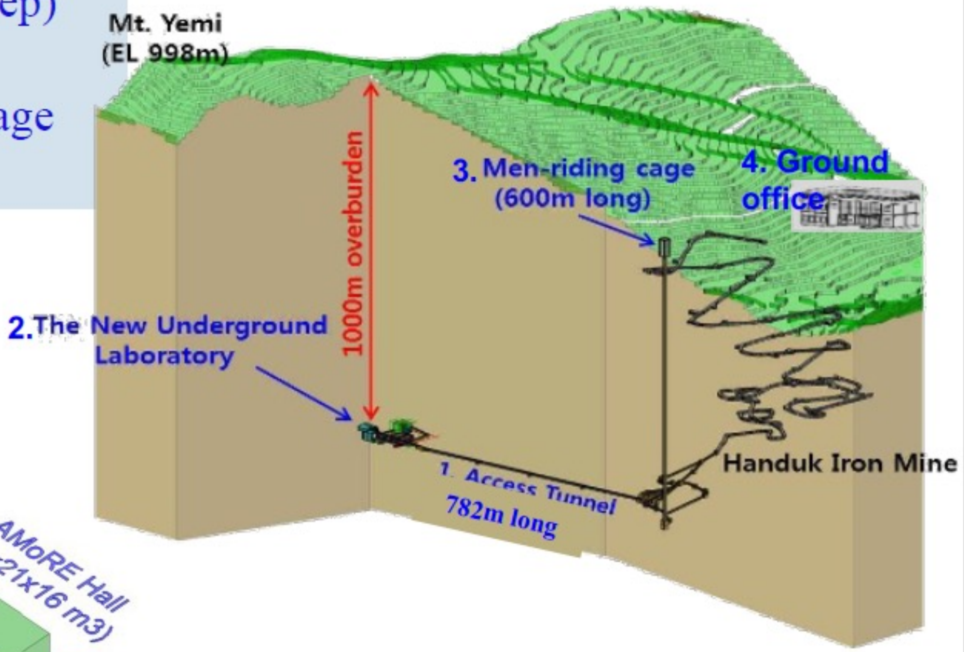

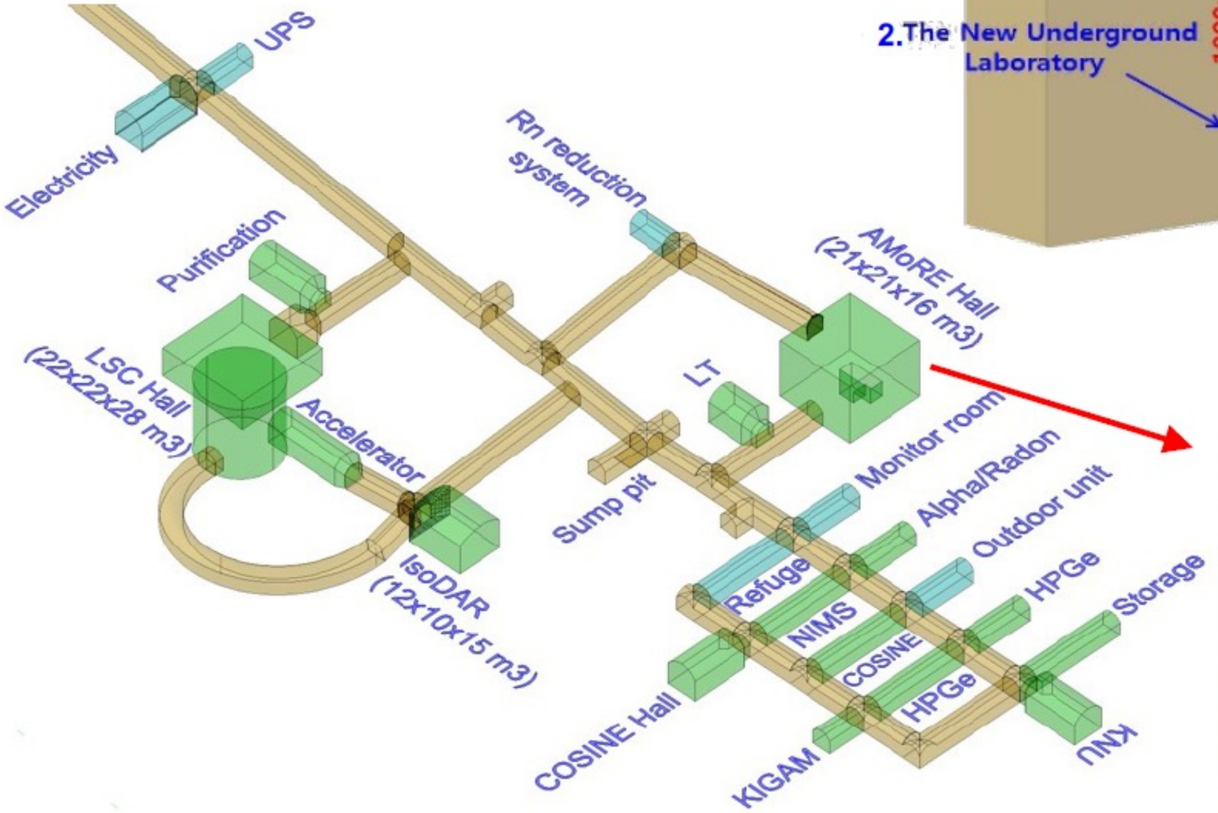

AMoRE-II detector

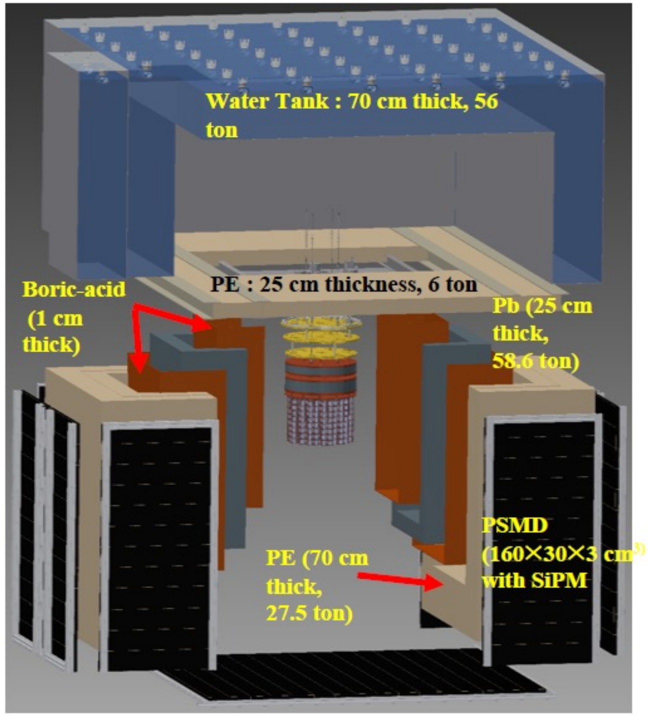

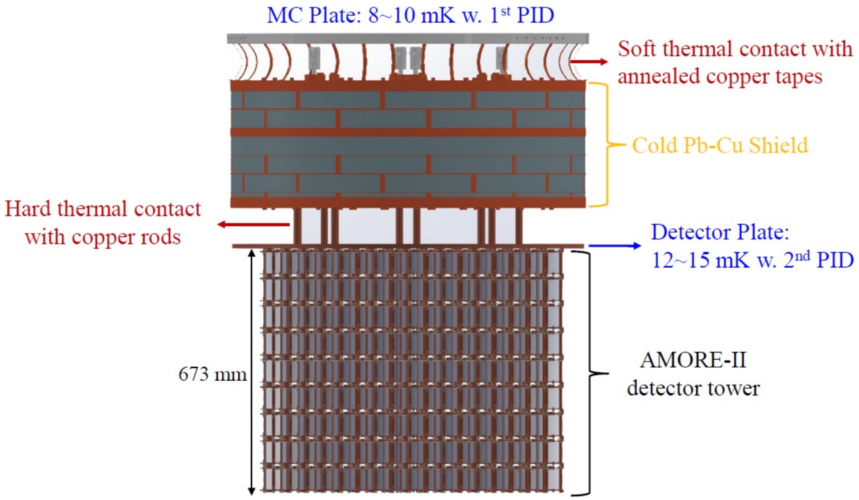

- The module designs are done for 5-cm and 6-cm LMOs.

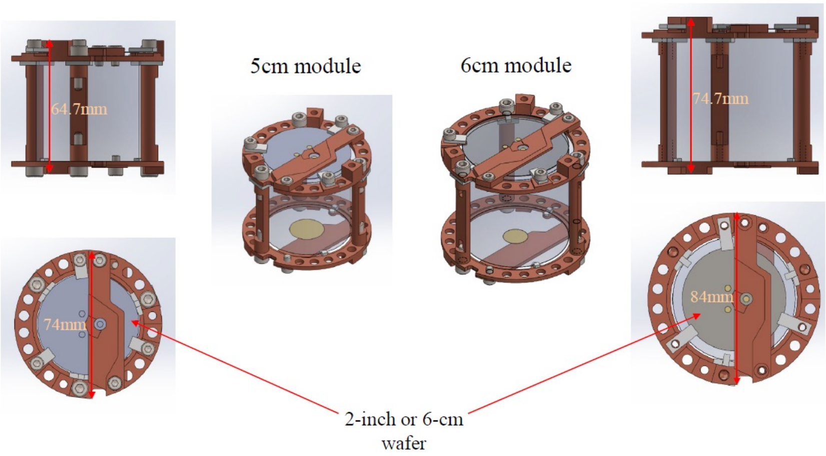

Preliminary

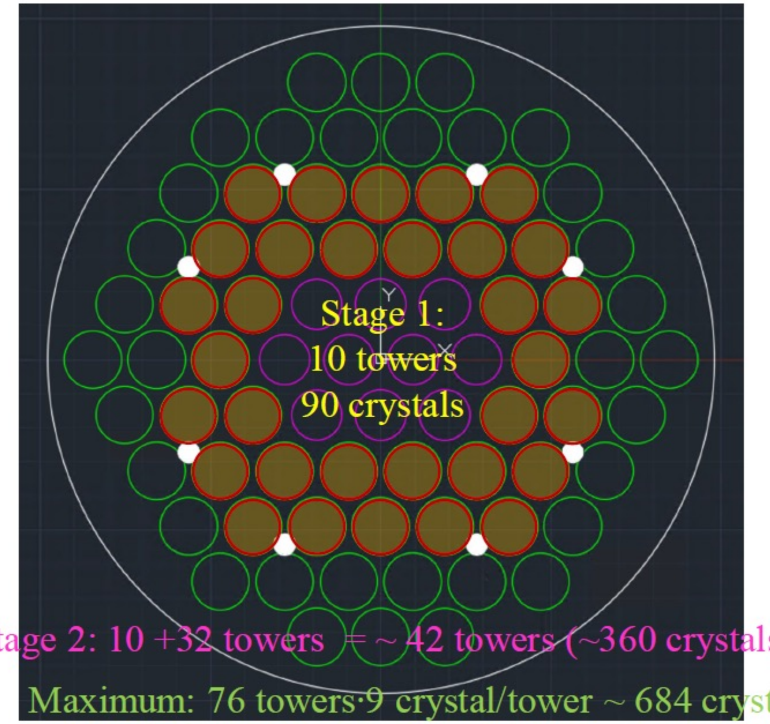

Stage 2: 10 +32 towers = ~ 42 towers (~360 crystals)

Maximum: 76 towers·9 crystal/tower ~ 684 crystals

Ultimate maximum: 50+26 towers·12 crystal/tower ~ 912 crystals

- LMO crystals: ∅5cm x H.5cm (310g) and ∅6cm x H.6cm (520g)
- Mass: ~80kg ^{100}Mo (~150kg crystal mass w. ~ 400 LMO crystals)

First Phase: 9 x10 ~ 24kg crystal mass

Limits & Sensitivities

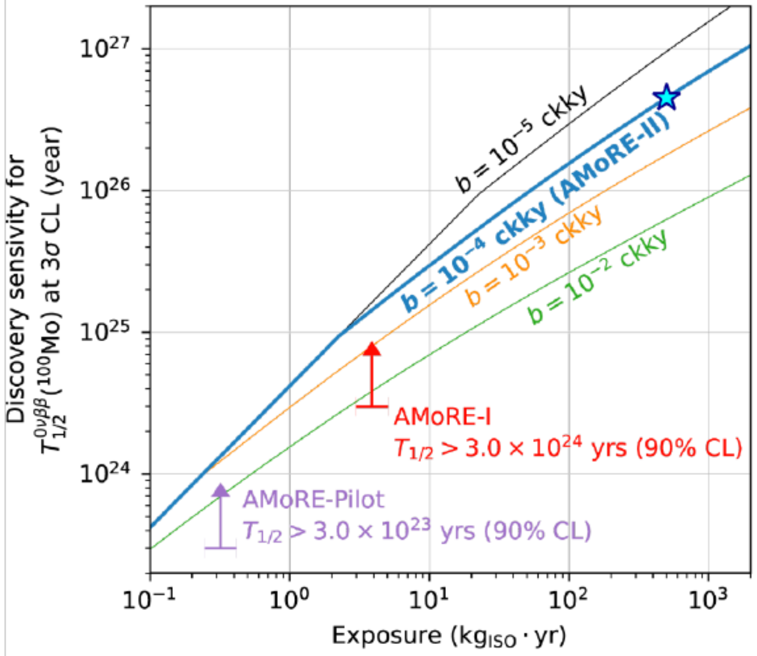

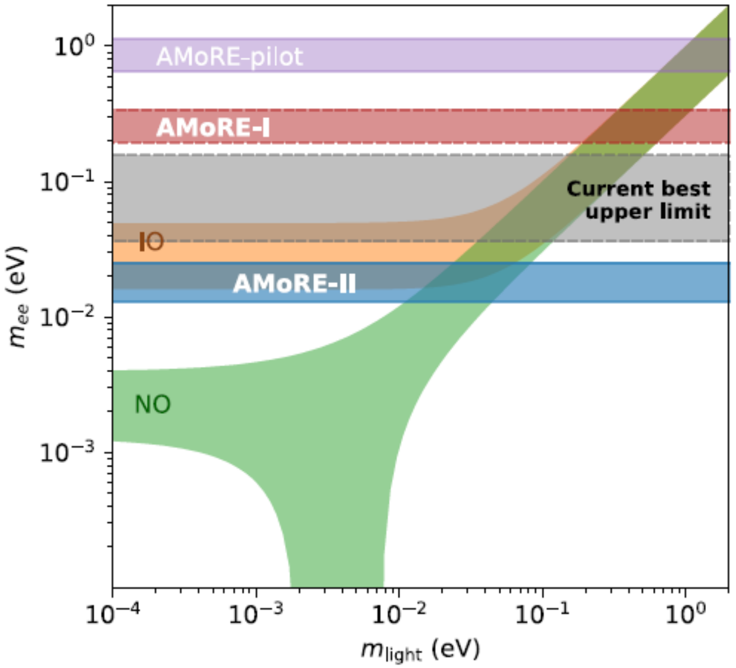

(By KamLAND-Zen Phys. Rev. Lett. 130 (2023) 051801)

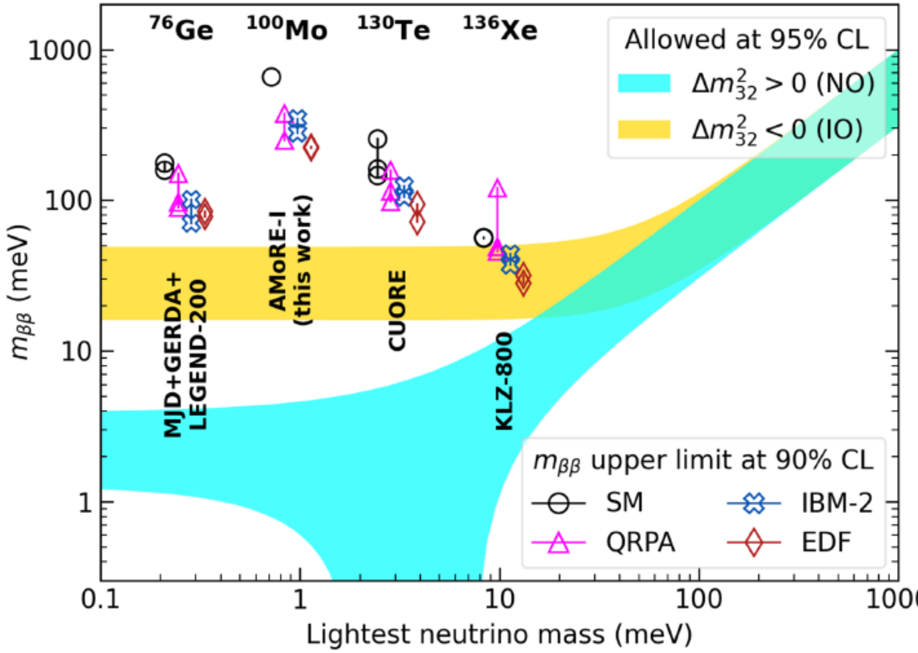

- AMoRE-I result corresponds to $m_{\beta\beta}$ <210-610 meV
- AMoRE-II for $T_{1/2}^{0\nu\beta\beta} > 4.4 \times 10^{26}$ years by 100 kg of ^{100}Mo × 5 years running.

  $m_{\beta\beta}$ <18-54 meV

Projected background and sensitivity of AMoRE-II, *Eur.Phys.J.C* 85 (2025) 1, 9

Thank you for your attention!

Back up slides

Background of AMoRE-II

Decomposing background in the ROI

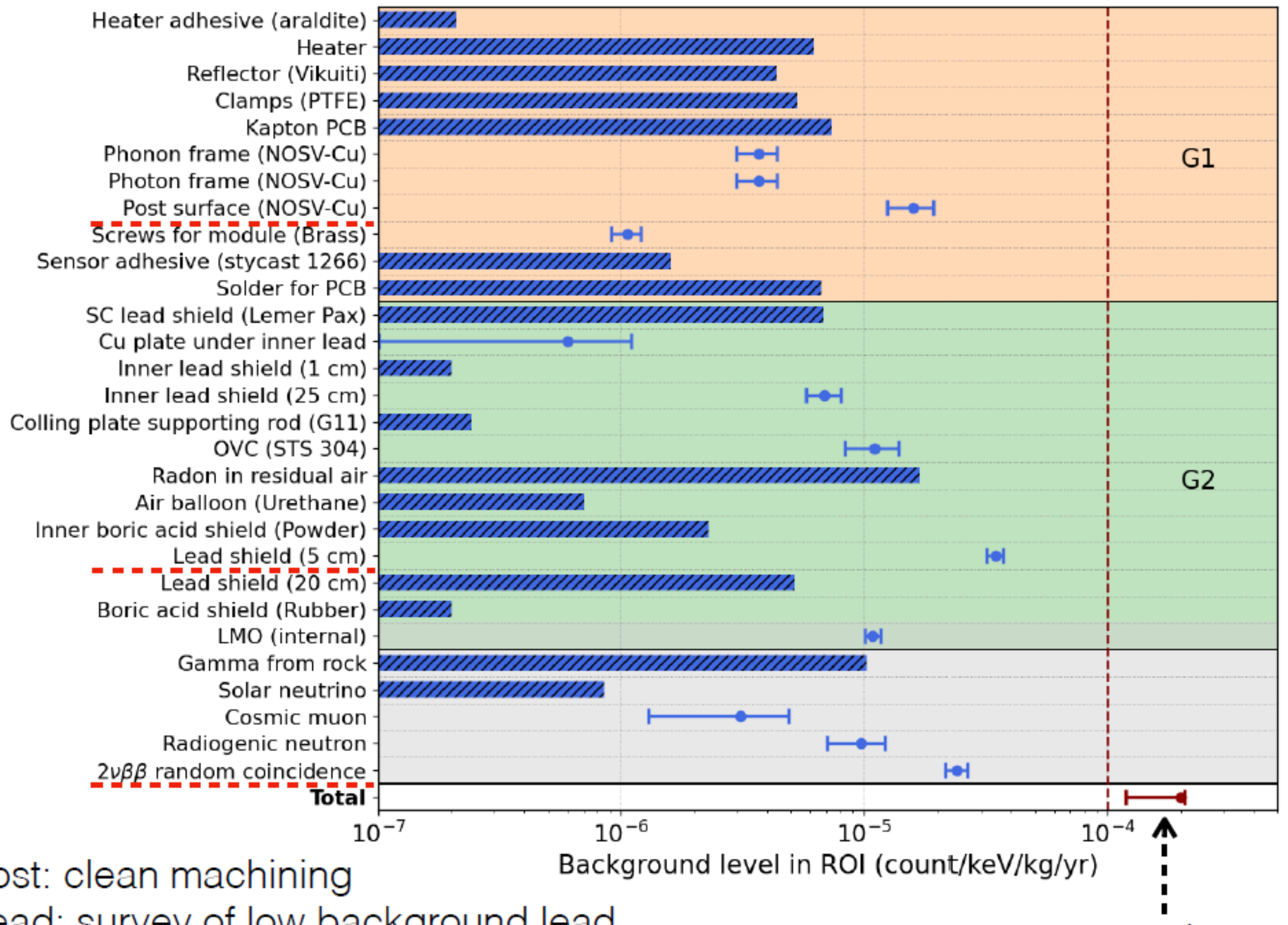

$(1-2)\times 10^{-4}$ cnts/keV/kg/year

Post: clean machining
Lead: survey of low background lead
$2\nu\beta\beta$ coincidence: inherent background

Cosmic ray muon background at YemiLab

❑ **Access tunnel with more overburden shortened to ~730 m by a simulation study considering a detail profile of the landscape.**

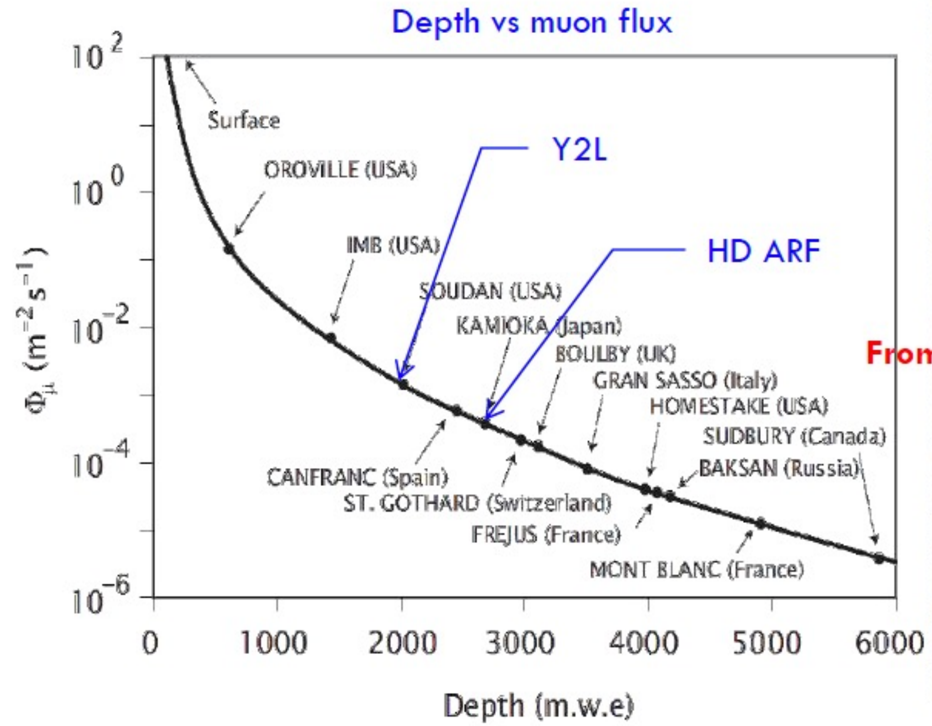

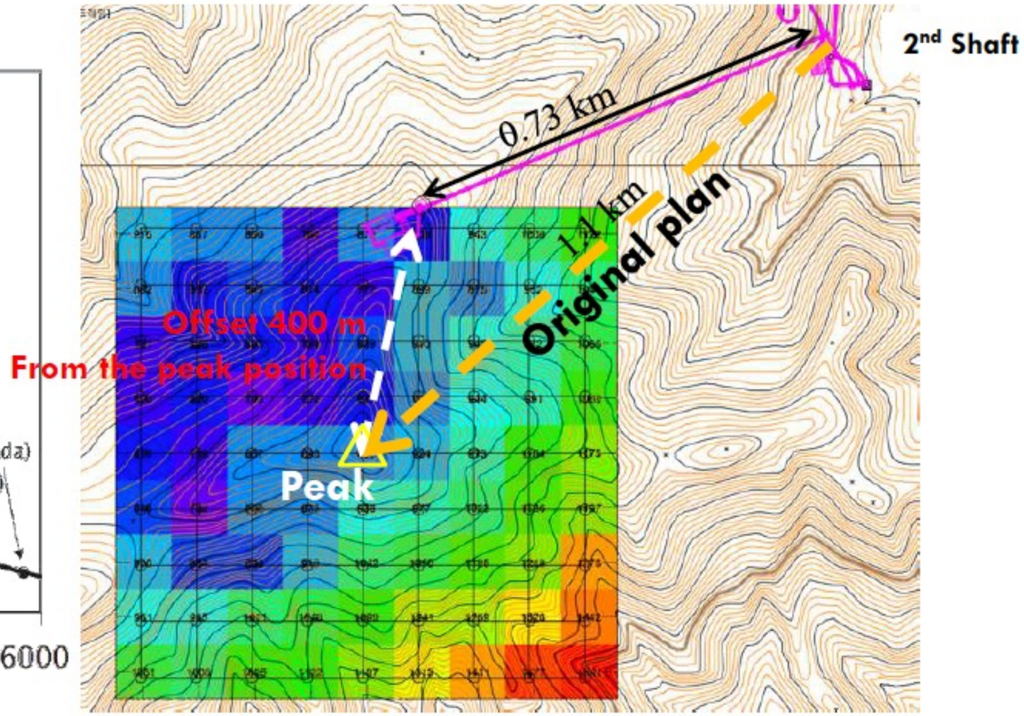

❑ **Muon reduction rate @ HD with a simulation: ~ 8 × 10^{-6}**

Energy Calibration – Bukin function

- Bukin function instead of gaussian/exponentially modified gaussian – better fit to right tails

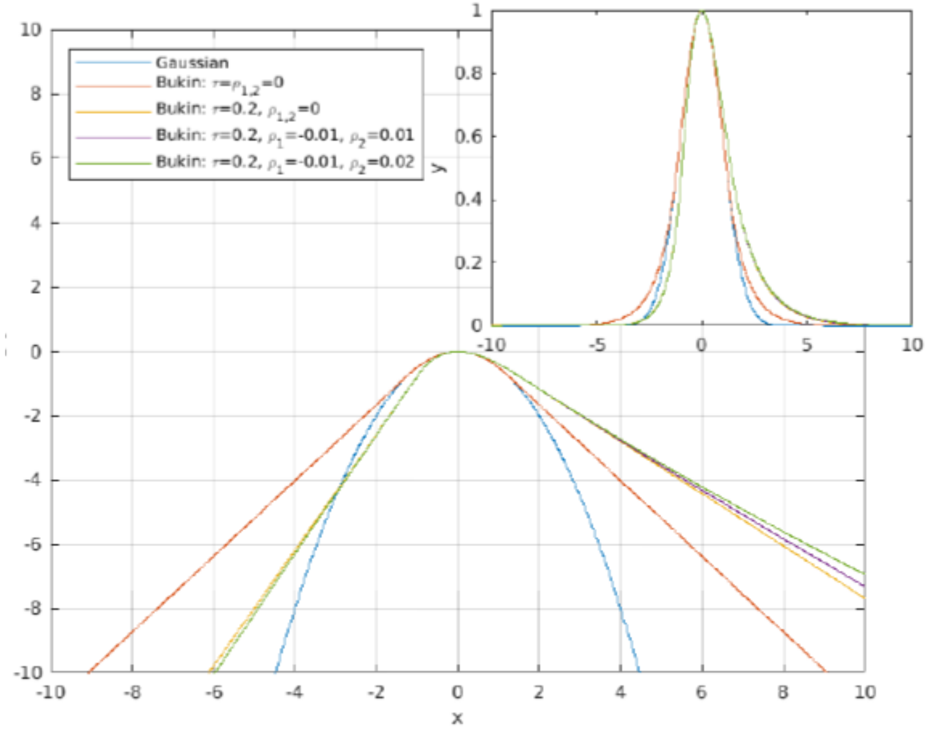

$$f_{\text{Bukin}}(x;\mu,\sigma,\tau,\rho_1,\rho_2) =$$

$$A\exp\begin{cases}\left[\dfrac{\tau\sqrt{\tau^2+1}(x-x_1)\sqrt{2\ln 2}}{\sigma(\sqrt{\tau^2+1}\quad\tau)^2\ln(\sqrt{\tau^2+1}+\tau)}+\rho_1\left(\dfrac{x-x_1}{\mu-x_1}\right)^2-\ln 2\right] & \text{if}\, x<x_1\\ \left[-\ln 2\left[\dfrac{\ln(1+\frac{2\tau\sqrt{\tau^2+1}(x-\mu)}{\sqrt{2\ln 2}\sigma})}{\ln(1+2\tau(\tau-\sqrt{\tau^2+1}))}\right]^2\right] & \text{if}\, x_1\le x<x_2\\ \left[-\dfrac{\tau\sqrt{\tau^2+1}(x-x_2)\sqrt{2\ln 2}}{\sigma(\sqrt{\tau^2+1}+\tau)^2\ln(\sqrt{\tau^2+1}+\tau)}+\rho_2\left(\dfrac{x-x_2}{\mu-x_2}\right)^2-\ln 2\right] & \text{if}\, x\ge x_2,\end{cases}$$

$$x_{1,2}=\mu+\sigma\sqrt{2\ln 2}\left(\frac{\tau}{\sqrt{\tau+1}}\mp 1\right) \qquad \text{(half maxima)}$$

- μ,σ: Gaussian mean & standard deviation, τ: asymmetry, $\rho_{1,2}$: left/right tail
- FWHM= $2\sqrt{2\ln 2}\,\sigma = x_2 - x_1$
- Become same as Gaussian when $\tau=0, \rho_{1,2}=-\ln 2$